

Collisional dissociation and chemical relaxation of alkali halide molecules: 2000–4200 K

Richard Milstein and R. Stephen Berry

Citation: *The Journal of Chemical Physics* **80**, 6025 (1984); doi: 10.1063/1.446684

View online: <http://dx.doi.org/10.1063/1.446684>

View Table of Contents: <http://scitation.aip.org/content/aip/journal/jcp/80/12?ver=pdfcov>

Published by the [AIP Publishing](#)

Articles you may be interested in

[Dissociation lifetimes of alkali halide dianions](#)

J. Chem. Phys. **110**, 5670 (1999); 10.1063/1.478465

[Clusters of alkali halide molecules](#)

J. Chem. Phys. **68**, 2159 (1978); 10.1063/1.436039

[Calculation of Collisional Dissociation of Alkali Halide Molecules by Classical OneDimensional Models](#)

J. Chem. Phys. **55**, 4628 (1971); 10.1063/1.1676799

[Curve Crossing in Collisional Dissociation of Alkali Halide Molecules](#)

J. Chem. Phys. **54**, 1752 (1971); 10.1063/1.1675082

[Chemical Overshoot: Thermal Dissociation of Alkali Halide Molecules](#)

Phys. Fluids **12**, I-118 (1969); 10.1063/1.1692589



Collisional dissociation and chemical relaxation of alkali halide molecules: 2000–4200 K

Richard Milstein and R. Stephen Berry

Department of Chemistry and the James Franck Institute, The University of Chicago, Chicago, Illinois 60637

(Received 3 October 1983; accepted 6 January 1984)

Shock-induced dissociation and the subsequent chemical relaxation processes of diatomic alkali halide molecules have been studied by time-resolved absorption spectrometry of alkali atoms, halide ions, and alkali halide molecules. The salts studied in detail are NaCl, KBr, RbCl, RbBr, CsCl, CsBr, and CsI. Rate coefficients have been determined in the temperature range 2000–4200 K for these processes: collisional detachment by argon $\text{Ar} + \text{X}^- \rightarrow \text{Ar} + \text{X} + e$; ionization of alkali atoms by thermal electron impact $e + \text{M}^0 \rightarrow 2e + \text{M}^+$; ion-ion neutralization $\text{M}^+ + \text{X}^- \rightarrow \text{M}^0 + \text{X}^0$; collisional dissociation to ions $\text{Ar} + \text{MX} \rightarrow \text{Ar} + \text{M}^+ + \text{X}^-$; and finally, collisional dissociation to atoms $\text{Ar} + \text{MX} \rightarrow \text{Ar} + \text{M}^0 + \text{X}^0$. The branching ratio (probability of dissociation to atoms)/(probability of dissociation to ions) is, in all cases studied, favorable to formation of ion pairs, relative to the equilibrium distribution of atom pairs/ion pairs. However, in every case except CsI, the primary collisional dissociation process gives a significant fraction of atom pairs.

INTRODUCTION

The dissociation and recombination processes of the diatomic alkali halide molecules have traditionally been prototypes for studying the molecular curve-crossing problem. The large electron affinities of the halogen atoms and the small ionization potentials of the alkali atoms put the energy of a widely separated ion pair only a little above the energy of the corresponding pair of neutral atoms in their ground state. The similarities among the systems of potential curves for the alkali halides, the variety of internuclear separations at which their crossings or avoided crossings occur, and the inherent appeal of the simple ionic-covalent picture make these molecules an ideal array for probing the relationships between molecular parameters and the degree to which the adiabatic noncrossing condition is satisfied. We have discussed this background in connection with the work which led to the investigations described here.^{1,2}

The dissociation and curve crossing processes of alkali halides have been inferred from the character of the molecular spectra.^{2–5} These processes have been studied more directly in time-resolved observations of shock-heated vapors;^{1,6–12} the work described here has pursued this line of attack. Finally, crossed beam studies of the collision process of rare gas atom with alkali halide have been undertaken.^{13–15} (We shall not discuss here the beam studies involving collisions of an alkali atom with a halogen atom; clearly these will be germane to any microscopic interpretation of the dissociation process.) The general situation has reached this point: it is clear that the dissociation of some alkali halide molecules, from their ground electronic states, produces an overwhelming preponderance of separated pairs of neutral atoms. This is the case for the lithium salts and for NaBr and NaI. It is also clear that many of the other alkali halides dissociate to give a nonequilibrium distribution of atom pairs and ion pairs; the actual ratios strongly favor the ion pairs, relative to the equilibrated distributions. If the time resolu-

tion of the measurements is high enough, then the ratio of atom pairs to ion pairs formed in the earliest stages of dissociation can be interpreted as the branching ratio for dissociation into the two channels. The actual values of these branching ratios have been the subject of some controversy. The measurements of the Chicago group,^{1,6} and of Mandl and co-workers,^{8–10} have been interpreted to indicate that the cesium salts, the rubidium salts (with the possible exception of RbI) and KCl and KF dissociate overwhelmingly to ion pairs of the form $\text{M}^+ + \text{X}^-$. The Göttingen results^{7,11} have been interpreted to mean that, although the relative concentration of ion pairs formed in the primary dissociation is far higher than at thermal equilibrium, quite generally many atom pairs are also produced in the primary dissociation step, even for the cesium salts. The beam experiments have shown that the cross sections for production of ion pairs are large enough to be entirely consistent with the interpretation that a large fraction of dissociating cesium and rubidium halides become ion pairs.

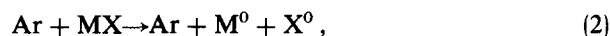
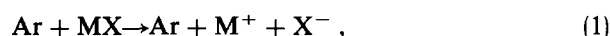
The measurements on which these various inferences are based are (with the exception of the beam experiments) spectrometric and time resolved. Mandl and co-workers monitored the absorption by F^- in its photodetachment continuum; the Göttingen group monitored the absorption by neutral molecules and halide ions or by a combination of neutral molecule absorption, and in a few cases, emission by excited alkali atoms; the Chicago group monitored absorption by neutral alkali atoms and by halide ions.

The alkali halides are an interesting set of systems in the temperature range discussed in this paper, roughly 2000–4200 K, because there are essentially only six species present apart from the carrier gas: the alkali halide MX, the neutrals M^0 and X^0 , the alkali ion M^+ , the halide ion X^- , and electrons. (A related paper¹⁸ gives results overlapping the upper end of this temperature range, extends to higher temperatures, and reviews the subject generally.) There are three constitutive equations, the mass balance for alkali, halogen,

and charge balance. Therefore, if the initial salt concentration is known, to complete the equations of mass balance, measurement of any three concentrations as functions of time completely determines the entire system. Amusingly, none of the groups working on this problem have heretofore made use of the full set of data that one can obtain from shock-heated, dissociating alkali halides, although there is a range of temperatures and concentrations where this is possible. It has been the purpose of this investigation to monitor the "complete" set of variables for as many alkali halides as we could, under as wide a range of temperatures and pressures as feasible, and to infer from these measurements the most consistent set of reactions and rate coefficients that we could find to describe these systems. In effect, we have looked, not at the kinetics of a single reaction, or at a single species in a series of related reactions, but at a set of interconnected reaction systems, with a presumably complete set of data for each reaction system. Moreover, we have attempted to describe not only the initial stages of dissociation, but the complete history of the reacting system for each shock-heated salt, from the beginning of the dissociation process to the attainment of chemical equilibrium. As we shall see, the constraints of such an elaborate analysis leave little room for alternative interpretations, at least at the level of unambiguous fitting of a set of phenomenological rate equations and rate coefficients. The relations between the rate laws that fit the observations and the interpretation of mechanism at the microscopic level are discussed in Ref. 18.

The salts we report here are NaCl, RbCl, CsCl, NaBr, KBr, RbBr, CsBr, RbI, and CsI. In all cases, the carrier gas was argon. For each shock, the concentrations of three species were measured by time-resolved absorption spectrometry: the neutral metal M^0 , the halide X^- , and the molecule MX. The experimental concentration profiles were compared with profiles based on the equations of a specific mechanism; the mechanism and its rate coefficients were varied until a satisfactory match could be produced between the experimental data and the theoretical model. The model was tested fairly extensively for possible multiple sets of solutions; only one physically reasonable mechanism and set of rate coefficients could be found to describe the data.

The kinetic model for this work is based on the following eight equations, and the corresponding reverse reactions:



Several other reactions were considered and eventually rejected. A more elaborate model is treated in Ref. 18, primarily because it deals with higher temperatures. The results provide rate coefficients for reactions (1)–(6). The rate coefficients for reactions (1), (2), and (3) are of order 10^{-15} cm^3/s ;

for the electron collision process (4), the rate coefficient is quite small, less than 10^{-13} cm^3/s ; reactions (5) and (6) have rate coefficients of order 10^{-10} and 10^{-11} cm^3/s , respectively. We shall consider these all in more detail in the discussion of results. First, however, it is appropriate to describe the experiments and the treatment of the data and of the model.

EXPERIMENTAL

The approach in this work is an extension of the shock tube technique we have employed previously.¹ Details of the tube and other basic equipment have been described previously,¹⁶ and the technique of operation is discussed in the doctoral dissertation upon which the present discussion is based.¹⁷ The tube itself has a square cross section with inside dimension of 3-1/2 in. on a side. Salt is introduced into the argon carrier gas as a smoke generated by heating a nichrome ribbon filament onto which the desired salt had previously been melted. The filament, flush with the tube wall, is about 4 in. from the end wall.

Experiments were carried out as follows. The smoke was prepared in the argon, so as to generate a concentration of about 0.1–0.01 mol% of salt in the carrier. The shock was released by a bursting diaphragm; its velocity was determined both by the pulses generated by its passage by three thermal resistance gauges (Pt painted on glass) and by the characteristic discontinuities produced by the shock front in the absorption spectra.

The incident shock vaporized the salt, usually without dissociating it. The reflected shock, returning into the shock-heated gas, dissociated the molecules. Under the conditions of our experiments, with temperatures behind the incident shock of 1000–2000 K, and with partial pressures well below 1 mm, no dimerization or polymerization occurs.

Time-resolved absorption measurements were used to monitor the neutral alkali atoms, the halide ions, and the neutral molecules. The atoms and negative ions were observed by photographic spectroscopy with a rotating-drum spectrograph, with a folded light path traversing the shock tube in an essentially horizontal direction (actually defining a thin slab). The technique for these measurements was described previously.^{1,16,17} Most measurements were made with four passes of the light beam. The lamp intensity was steady after the first 25 μs ; the duration of the absorption source was about 200 μs .

Molecular absorption was studied with a 150 W Hanovia xenon lamp as a source, filtered through an interference filter with a 300 Å bandpass around 2500 Å. This region is one in which both molecules and halide ions absorb, but in which the molecular absorption is strong enough¹⁹ that one obtains meaningful data on molecular concentrations after the contribution from negative ions is subtracted from the raw data. The negative ion absorption measurements were obtained in the regions near the thresholds, where molecular absorption is negligible and the interpretation of the continuous absorption is unambiguous. The intensity of the filtered light was monitored with an RCA 1P28 photomultiplier and displayed on an oscilloscope (Tektronix 545B).

The total time resolution for measurements of concentration was 2 μs or better. Molecules could be observed for at

least 15 μs in the region behind the incident shock. This is long enough that the molecules experience several hundred thousand collisions, so that it is a very good assumption to suppose that vibrational equilibration occurs in this region.

DATA ANALYSIS

The spectroscopic data were reduced by taking microdensitometer scans of intensity as a function of wavelength, at intervals corresponding to 2 μs of laboratory time (and to time in the gas behind the reflected shock as well) to 16 μs , and at 4 μs intervals thereafter, following the reflected shock front. Each batch of film was calibrated with a seven-step neutral density filter. The spectral scans were deconvoluted according to the method of Brodersen,^{20,21} with the assumption that the lines are Lorentzian; the slit function was assumed to be triangular and the width of this function was determined by measuring the widths of instrumentally broadened krypton lines.

The molecular absorption was obtained by subtraction of the halide concentration, based on the photographic measurements, from the photoelectrically measured absorption in the 2500 Å region. A separate measurement of this sort was necessary to find the third concentration because the range of the spectrograph was only sufficient to permit the metal atom and halide ion concentrations to be measured, when the dispersion was high enough to permit the alkali absorption lines to be used to determine concentrations.

The experimental points were fit, for later computational convenience, with simple functions; the halide concentrations were represented with three exponentials, the metal atom concentrations with two exponentials, and the molecular concentrations, with Chebyshev polynomials. In all cases the least-square fits were well inside the experimental scatter and precision of the measurements. Typically, the deviations from the mean square percentage deviation δ_f were between 5% and 10% for the alkali atoms and halide ions, and between 1% and 5% for the molecules.

We have previously noted that our systems consist of six species in addition to the argon carrier gas: MX , M^0 , X^0 , M^+ , X^- , and e . At all times, these constitutive equations apply:

$$[e] + [\text{X}^-] = [\text{M}^+], \quad (9)$$

$$[\text{MX}]_{t=0} = [\text{MX}] + [\text{X}^-] + [\text{X}^0], \quad (10)$$

and

$$[\text{MX}]_{t=0} = [\text{MX}] + [\text{M}^+] + [\text{M}^0]. \quad (11)$$

At equilibrium, three more equations must be satisfied:

$$K_1 = \frac{[\text{M}^0][\text{X}^0]}{[\text{MX}]}, \quad (12)$$

$$K_2 = \frac{[\text{M}^0][\text{X}^0]}{[\text{M}^+][\text{X}^-]}, \quad (13)$$

and

$$K_3 = \frac{[\text{X}^0][e]}{[\text{X}^-]}. \quad (14)$$

Thus, determination of only *one* concentration at equilibri-

um, or of the constant $[\text{MX}]_{t=0}$, the total salt concentration behind the reflected shock, fixes all other quantities when equilibrium is reached.

The photoabsorption cross sections have been reported for the halide ions²²⁻²⁴ and the alkali halide molecules,¹⁹ as have oscillator strengths for the alkali lines.²⁵⁻²⁹ Our observations of these three species therefore constitute three independent measurements, each of which is sufficient to determine the concentrations of all the species at equilibrium. Hence the system is well overdetermined, and we can examine the mutual consistency of the absorption cross sections and oscillator strengths.

The details of the investigation of oscillator strengths and absorption coefficients are given in the Appendix. In general, we found that the molecular and halide ion absorption cross sections are consistent with each other and with the data, but that the published values of some of the oscillator strengths for the alkali atomic lines were not consistent with the rest of our data. We selected a "most self-consistent" set of absorption coefficients and oscillator strengths, and, from these, determined the concentrations. The halide ion cross sections are, within the uncertainties of our experiments, those given by Steiner, Seman, and Branscomb^{22,23} and by Rothe.²⁴ This is reassuring, because these determinations are based on very different methods, yet give consistent results. Moreover, the extinction curves of the halide ions are very flat for long intervals including the ranges of wavelength in which our measurements were made, so that the instrumental artifacts and difficulties associated with intensities of lines do not affect the measurements. Finally, the halide ion absorption coefficients are presumably independent of temperature, so that the problems of temperature dependence that might arise with the molecular absorption are not present for the halides. We therefore ultimately used the halide ion absorption cross sections as one primary standard for determining concentrations. Cross sections typical of those we took for the halide ions are: Cl^- ; $2 \times 10^{-17} \text{ cm}^2$ at 3200 Å; Br^- ; $2 \times 10^{-17} \text{ cm}^2$ at 3400 Å, and I^- ; $2.2 \times 10^{-17} \text{ cm}^2$ between 3200 and 3800 Å. The data are best summarized in Ref. 24.

The molecular absorption cross sections at 2500 (± 150) Å that we derived are given in Table I, together with the values measured by Davidovits and Brodhead.¹⁹ Table II gives our derived values for oscillator strengths of the alkali lines we used, together with values reported previously.

TABLE I. Molecular absorption cross sections at 2500 Å.

Salt	$\sigma(\text{cm}^2) \times 10^{-11}$	
	This work	Ref. 19
RbCl	1.21 ± 0.31	1.22
CsCl	1.6 ± 1.0	0.95
KBr	1.25 ± 0.60	1.25
RbBr	1.37 ± 0.51	1.37
CsBr	1.35 ± 0.20	2.17
RbI	1.90 ± 0.85	3.70
CsI	5.3 ± 3.6	3.56

TABLE II. Absorption oscillator strengths for spectral lines of alkali atoms.

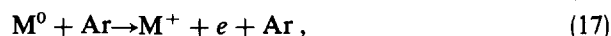
Atom	Transition	f : This work	Other values
K	$6p \leftarrow 4s$	$(1.73 \pm 0.70) \times 10^{-4}$	2.25×10^{-3a}
			8.23×10^{-4b}
Rb	$7p \leftarrow 5s$	$(3.8 \pm 1.7) \times 10^{-4}$	3.7×10^{-3a}
			1.87×10^{-3b}
			2.103×10^{-3c}
Rb	$8p \leftarrow 5s$	$(2.00 \pm 0.33) \times 10^{-4}$	5.513×10^{-4b} 1.28×10^{-3c}
Cs	$9p \leftarrow 6s$	$(2.6 \pm 1.3) \times 10^{-3}$	5.363×10^{-4b}
			8.603×10^{-4d}
			1.25×10^{-3e}
			3.83×10^{-5f}
Cs	$10p \leftarrow 6s$	$(1.23 \pm 0.19) \times 10^{-4}$	2.284×10^{-4b}
			4.684×10^{-4e}
			6.49×10^{-4e}

^a Reference 28.^d Reference 26.^b Reference 49.^e Reference 29.^c Reference 27.^f Reference 25.

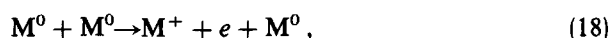
KINETIC MODELING

The Eqs. (1)–(8) and the corresponding reverse reactions define the basic set of processes in our model. The branching ratio for dissociation into the atomic and ionic channels is equal to the ratio k_2/k_1 of the “forward” rate constants for reactions (2) and (1).

Additional reactions were considered and were eventually dropped. These excluded reactions are



and



and the corresponding reversed reactions. The grounds for excluding these were as follows. Reactions (15) and (16) will compete with reaction (3), $Ar + X^- \rightarrow Ar + X + e$, but the thousandfold or ten thousandfold excess of argon over X^0 , even at equilibrium, will make reactions (15) and (16) insignificant by comparison with reaction (3), even if the rate coefficients for (15) and (16) are somewhat larger than those for reaction (3). As we shall see, the rate coefficients for reactions of the type (3) are, according to our results, about the same magnitude as those expected^{30–34} for such processes as $H + H^- \rightarrow 2H + e$, or $O + O^- \rightarrow 2O + e$, analogous to reaction (15), and comparable to those found for detachment of electrons from negative alkali ions in collisions with rare gas atoms.³⁵ Moreover the only distinction between processes (15) and (16) is the free or bound character of the final state describing the relative motion of the heavy nuclei, and the mean cross section for associative electron detachment (16) is, if anything, smaller than that for the collisional process (15).

Process (17) was omitted on the basis of the measurements by Haught of the rate of ionization of Cs in argon.³⁶ In those experiments, it was found that argon–cesium collisions

made a negligible contribution to the ionization process, that process (18) generated the first few electrons, and that process (6) was responsible for almost all the ionization of cesium. In our system, process (3) generates electrons far faster than process (18), so that we cannot expect to get any measurable contribution from process (18), and therefore neglect it.

The process



was omitted because, according to Zel'dovich,³⁷ “this process is of importance only for extremely low degrees of ionization, less than 10^{-7} – 10^{-10} .” In our system, the three-body recombination of electrons with positive ions is achieved essentially entirely by the reverse of process (6), in which electrons act as the third body.

The processes that were kept in the scheme call for a little comment. Dissociative attachment (7) was included because this process does appear to play an important role in dissociation of the hydrogen halides.³⁸ The rate for process (8) is quite unknown, but we can expect that if dissociative attachment is important, then the corresponding process that leaves the electron in a free final state will become even more important when the effective temperature or collision energy is high enough to open the channel for process (8). Moreover the scattering cross sections for electrons by alkali halides are large.³⁹ Finally, the charge exchange process (5) is included because of the known large cross sections for ion–ion neutralization.^{40,41}

The modeling process was carried out almost entirely on a Beckman EASE model 2132 analog computer. (A digital method, based on a steepest-descent approach to a least-squares fit, was attempted. However this technique turned out to be unreliable because of large numbers of local minima in the function space that could only be sorted from true solutions by painstaking case-by-case comparisons with the data and with other solutions.) The use of the analog computer for solving our coupled rate equations is described in detail elsewhere; the techniques are standard. The data from each shock is treated independently. One arrives at a set of rate coefficients for a chosen shock by varying a set of potentiometers to obtain a best visual fit of the modeled rates to the experimental data, and then reads the rate coefficients off as values of the potentiometer settings. Best visual fits were obtained by graphing suitably scaled curves of the experimental data on transparent mylar sheets, taping these graphs onto the output display tube (iterative differential analyzer display or IDAD) and matching the output curves on the IDAD to the super-imposed graph. This way, all three curves, for $M^0(t)$, $X^-(t)$, and $MX(t)$ taken from a single shock, could be fit simultaneously. It turned out that the capability to fit all three curves at once was very important in eliminating false solutions. When optimum solutions were found, the potentiometer settings were recorded and the solutions were plotted on the conventional output chart of an x - y plotter linked to the analog computer. Finally, the accuracy of the fit was determined by a comparison (on a digital computer) of the curves generated by the model and the experimental points themselves.

The experimental data could, in general, be fit by only a

narrow range of rate coefficients. However the fits did generally lie well within the experimental error. In many cases, it was possible to get more than one satisfactory fit to one or even, in some cases, to two concentration curves for a given shock. However it was only possible to find a single fit for all three curves, for all the shocks we studied this way (29 with all three species, and an additional 9 with only two species measured, as checks). It was sometimes rather a problem to find the one set of constants that did fit the data.

Only after a preliminary collection of rate coefficients was obtained, one set from each shock being analyzed, were the rate coefficients examined for consistency. This comparison then enabled us to obtain a better set of values, which turned out, after iteration, to be essentially the final set.

RESULTS OF THE ANALYSIS

A. Modeling

Typical fits of the modeled concentration curves to the experimental data are shown in Figs. 1–4. The quality of the fitting was estimated by a chi-square analysis as well as by direct evaluation of the percent deviation δ_m of the experimental points from the modeled curves. Here, δ_m is defined just as δ_f was; except that the values on the model curves replace those from the directly fitted curves. It was generally possible to obtain almost as good values for δ_m as it was for δ_f . Moreover it was generally possible to obtain at least two shocks for each salt for which χ^2 gave confidence limits of 70% or higher for all three curves, fitted simultaneously. In some cases, the χ^2 for one concentration curve, usually MX, would imply a very low confidence limit. Invariably in such cases it would turn out that the experimental points and model curve for the errant variable would be virtually parallel, deviating in a *systematic* way. Attempts to improve the fits in such cases were unsuccessful, and we were forced to assume that a systematic error had caused the deviation and the low confidence limit. Despite these apparent difficulties, the rate coefficients associated with the fits with low confidence limits are still rather close to those from the more

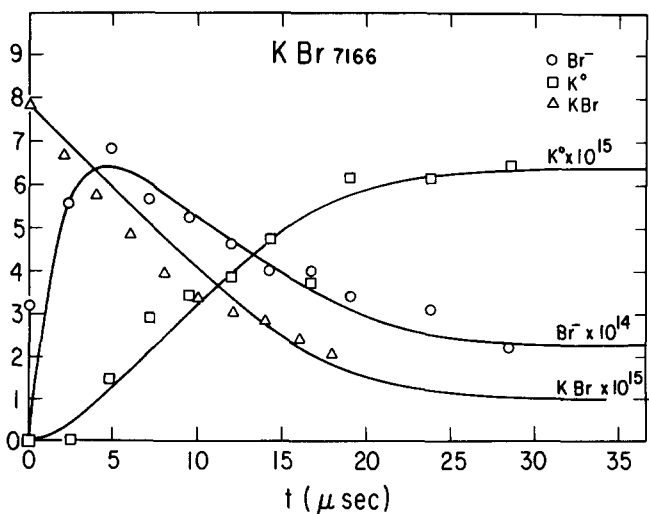


FIG. 1. Experimental points and modeled concentration curves for a typical shock with KBr in argon (shock no. 7166).

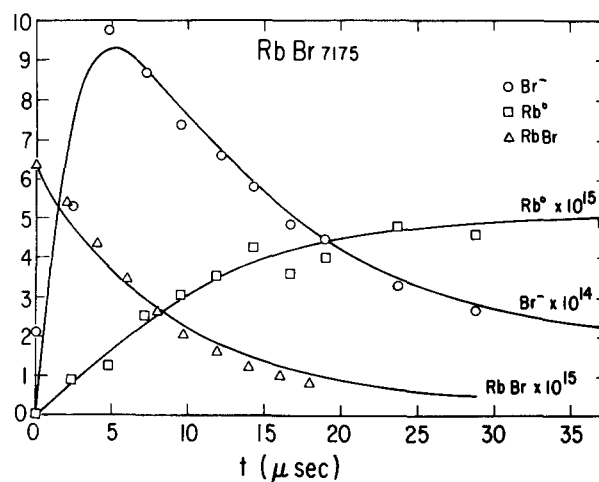


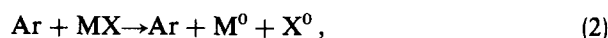
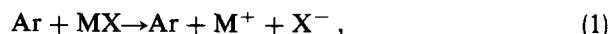
FIG. 2. Experimental points and modeled concentration curves for RbBr (shock no. 7175).

satisfactory curves. The values of χ^2 , δ_m , and δ_f are given in Ref. 17.

We attempted to fit the data with very small or zero values for the rate coefficient of reaction (2), corresponding to collisional dissociation to atoms. This was the best way to match the data for CsI, but for all the other salts reported here, it was not possible to neglect reaction (2). When this reaction was omitted, the data at early times, 0–3 μ s following the reflected shock, could be reproduced but the concentrations calculated for later times bore no resemblance to the observed data.

B. Rate coefficients

Rate coefficients were determined for these reactions:



and

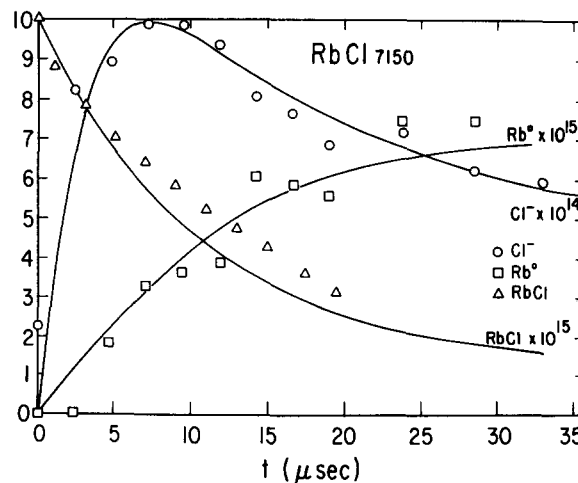


FIG. 3. Experimental points and modeled concentration curves for RbCl (shock no. 7150).

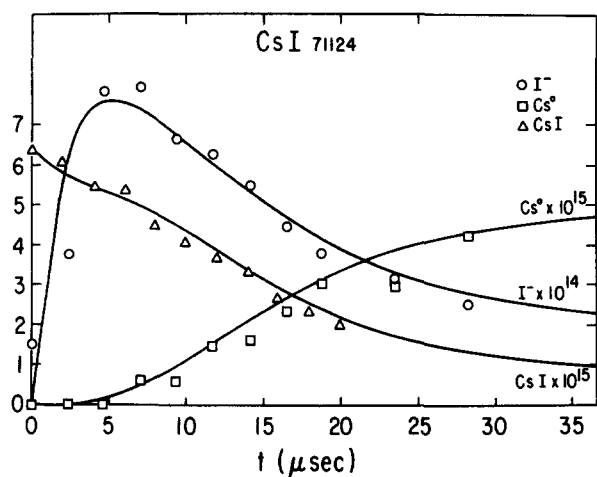


FIG. 4. Experimental points and modeled concentration curves for CsI (shock no. 71124).



An upper limit of 10^{-13} cm³/s was found for the rate coefficient of the reaction



for X = Cl, Br, and I. (The cross section for the analogous reaction with X = H was found to be $\sim 4 \times 10^{-15}$ cm² at 8.9 eV,⁴² but the extrapolation to thermal energies is extremely hazardous.)

The reactions (1) and (2) were fit to Arrhenius plots with

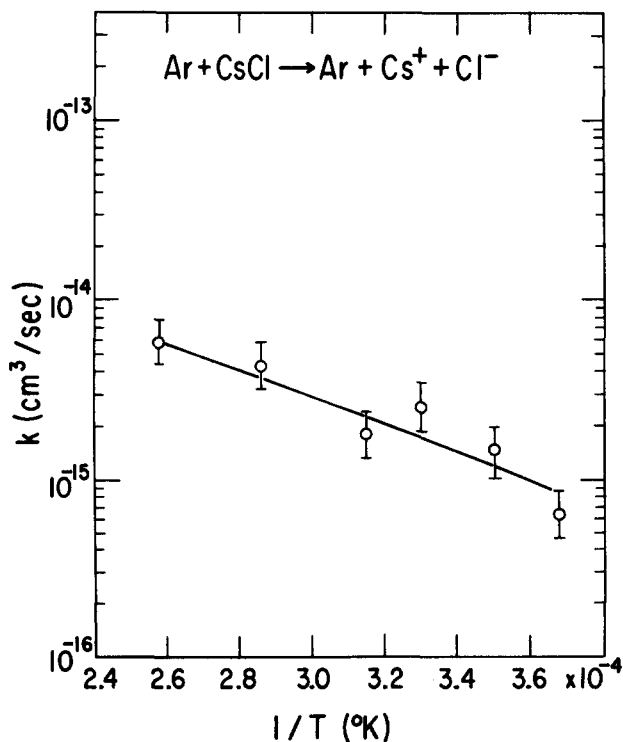


FIG. 5. Arrhenius plot for the collisional dissociation of CsCl to ions, according to reaction (1).

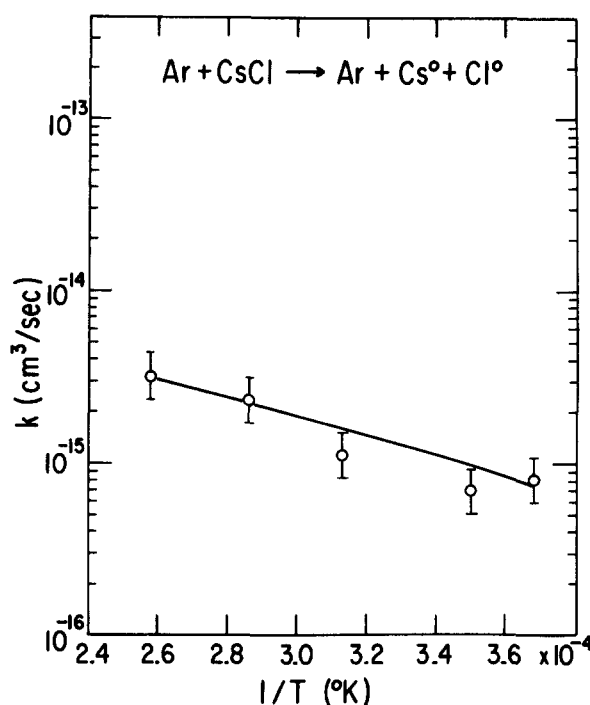


FIG. 6. Arrhenius plot for the collisional dissociation of CsCl to atoms, according to reaction (2).

the form derived by Mandl⁹ from the theory of Bates and Flannery⁴³

$$k = AT^{-7/2} \exp(-E/kT).$$

Other rates were fit to the form $k = A \exp(-E/kT)$. The various data points were weighted in the Arrhenius plots according to their values of χ^2 . Typical Arrhenius plots are shown in Figs. 5–7 for reactions (1) and (2), in Figs. 8–10 for reaction (3), and in Fig. 11 for reaction (6). A full set of plots and tables of the kinetic data for these and other relevant

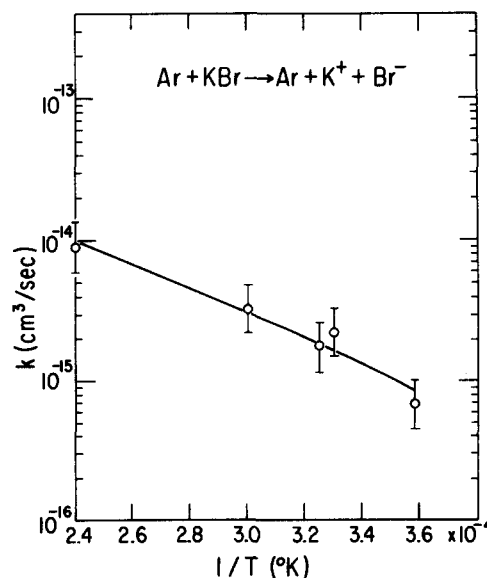


FIG. 7. Arrhenius plot for the collisional dissociation of KBr to ions, according to reaction (1).

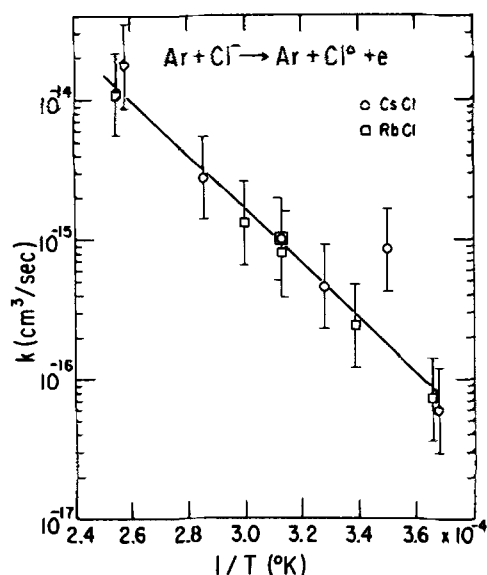


FIG. 8. Arrhenius plot for detachment of electrons from Cl^- by collisions with Ar, based on shocks in CsCl and RbCl.

experiments with rubidium and cesium halides is given in Ref. 18. Note that the plots for detachment and ionization processes (3) and (6) (except for the I^- detachment reaction) include data from more than one salt. The internal self-consistency of the data from different substances has been strong reinforcement for our acceptance of the validity of the rate coefficients, the activation energies and the model itself.

C. Collisional detachment

The rate coefficients and activation energies for the collisional detachment reaction (3) are collected in Table III, at the temperatures for which the rates are most reliable. In the Arrhenius form, we obtain

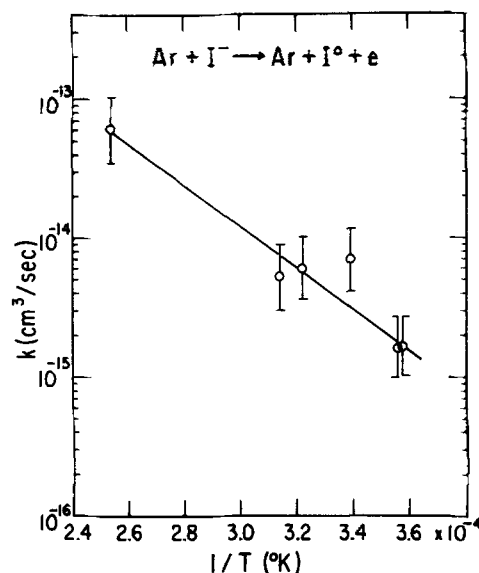


FIG. 10. Arrhenius plot for detachment of electrons from I^- by collisions with Ar, based on data from CsI.

$$k(\text{Cl}^-) = 9.64 \times 10^{-10} \exp(-87.8/RT),$$

$$k(\text{Br}^-) = 3.59 \times 10^{-11} \exp(-59.4/RT),$$

and

$$k(\text{I}^-) = 3.51 \times 10^{-11} \exp(-67.8/RT).$$

(Preexponentials are in cm^3/s ; activation energies are in kcal.) The measured activation energies for Cl^- and I^- are close to the electron affinities of the respective atoms (83.69 and 71.00 cal, respectively) but the measured bromide activation energy is about 25% lower than the 77.92 cal electron affinity of Br. This is within the uncertainty of our determination of the activation energy.

Collisional detachment rate coefficients were reported

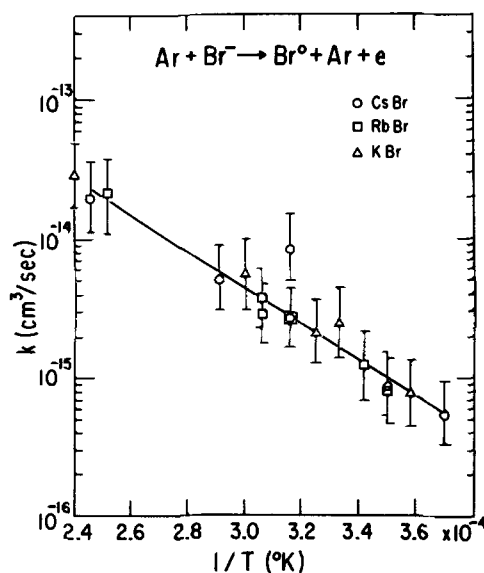


FIG. 9. Arrhenius plot for detachment of electrons from Br^- by collisions with Ar, based on data from KBr, RbBr, and CsBr.

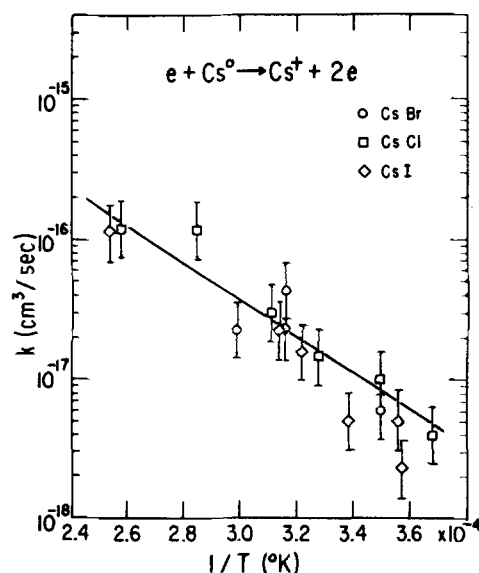


FIG. 11. Arrhenius plot for ionization of Cs^0 by electron impact, based on data from CsCl, CsBr, and CsI.

TABLE III. Rate coefficients and activation energies ΔE for the apparent reaction (3), $\text{Ar} + \text{X}^- \rightarrow \text{Ar} + \text{X}^0 + e$. (This process is discussed in detail, particularly regarding the microscopic interpretation of these rate coefficients, in Ref. 18.)

Ion	T	k (this work)	k (Ref. 11)	ΔE (this work)	ΔE (Ref. 11)
Cl^-	3200 K	$9.7 \times 10^{-16} \text{ cm}^3/\text{s}$	7.1×10^{-16}	87.8 kcal/mol	83.0
Br^-	3000	4×10^{-15}	7.3×10^{-16}	59.4	78.0
I^-	2400 3125	2.3×10^{-16} 6×10^{-15}	$< 5 \times 10^{-16}$ $(1.4 \times 10^{-14},$ calculated from A and $\Delta E,$ as given.)	67.8	70.6

by Luther, Troe, and Wagner.¹¹ Their values are incorporated in Table III, for the appropriate temperatures; in the Arrhenius form, their rate coefficients are

$$k(\text{Cl}^-) = 3.3 \times 10^{-10} \exp(-83.0/RT),$$

$$k(\text{Br}^-) = 3.5 \times 10^{-10} \exp(-78.0/RT),$$

and

$$k(\text{I}^-) = 1.2 \times 10^{-9} \exp(-70.6/RT).$$

These values are not seriously inconsistent with our own. To illustrate the sorts of uncertainties associated with these determinations, we note that Mandl, Kivel, and Evans,^{8(b)} measuring the collisional detachment rate for $\text{Ar} + \text{F}^-$, found that at 4500 ± 150 K, they obtained detachment rate constants ranging from 8×10^{-16} to 5×10^{-15} .

D. Charge exchange

The temperature dependence of the rate of reaction (5) is small, as one expects in an exothermic process. The rates themselves, of order $10^{-10} \text{ cm}^3/\text{s}$, are listed in Table IV, for a temperature of 3000 K. The effective cross sections, defined by the approximation $\sigma_{\text{eff}} = k/v_{\text{mean}}$ and the mean relative velocity v_{mean} are also tabulated. These cross sections are much smaller than cross sections for ion-ion neutralization, as in the $\text{Na}^+ + \text{O}^-$ process, for example,^{40,41,44} which are in the range of 10^{-13} cm^2 . This discrepancy is not easy to understand, although there are differences between the systems that may help to account for the small cross sections in the case of the alkali halides. First, the alkali halides exhibit crossings (or avoided crossings) of their ionic potential curves with the potential curves correlating to the ground configurations of their separated atoms, while the systems,

TABLE IV. The rate coefficient and effective cross sections for reaction (5) $\text{M}^+ + \text{X}^- \rightarrow \text{M}^0 + \text{X}^0$ at 3000 K.

Salt	$k_s(\text{cm}^3/\text{s})$	$v(\text{cm}/\text{s})$	$\sigma_{\text{eff}}(\text{cm}^2)$
RbCl	2.0×10^{-10}	1.74×10^5	1.0×10^{-15}
CsCl	3.0×10^{-10}	1.64×10^5	2.0×10^{-15}
KBr	2.5×10^{-10}	1.69×10^5	1.5×10^{-15}
RbBr	1.5×10^{-10}	1.35×10^5	1.0×10^{-15}
CsBr	2×10^{-10}	1.22×10^5	1.5×10^{-15}
CsI	2.5×10^{-10}	1.07×10^5	2.5×10^{-15}

such as $\text{Na}^+ - \text{O}^-$, $\text{O}^+ - \text{O}^-$, and $\text{H}^+ - \text{H}^-$ that have been studied for their ion-ion neutralization cross sections, exhibiting crossings of their ionic curves with curves corresponding to excited configurations of the separated neutral atoms. Second, the largest separation of a crossing point for the alkali halide ground state is 51 \AA (for CsCl) while the other systems exhibit some much larger crossing distances, 288 \AA for



a process shown to be very important in the $\text{Na}^+ - \text{O}^-$ neutralization mechanism.⁴¹ Presumably the smaller orbitals and the more restricted ranges of interaction, i.e., the narrower ranges in which the initial and final electronic states are nearly degenerate, are responsible for the small cross sections of the alkali-halogen ion pairs toward reaction (5). Despite the small values of about 10^{-15} for the rate coefficient, reaction (5) does, nonetheless, play a significant part in the time dependence of both M^0 and X^- .

E. Collisional ionization

It proved necessary to include the collisional ionization by electron impact,



in our scheme, in order to fit the concentration curves. The rate coefficients k_6 at a temperature of 3200 K, are

$$1.2 \times 10^{-11} \text{ cm}^3/\text{s} \text{ for K,}$$

$$9.0 \times 10^{-12} \text{ cm}^3/\text{s} \text{ for Rb,}$$

$$2.3 \times 10^{-11} \text{ cm}^3/\text{s} \text{ for Cs.}$$

When the rates are fit to Arrhenius plots, we obtain

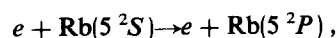
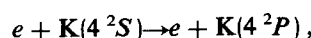
$$k_6(\text{K}^0) = 1.21 \times 10^{-4} \exp(-102.1/RT),$$

$$k_6(\text{Rb}^0) = 2.00 \times 10^{-8} \exp(-48.7/RT),$$

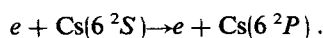
and

$$k_6(\text{Cs}^0) = 3.45 \times 10^{-7} \exp(-60.2/RT).$$

The only comparable results for thermal electrons appear to be the rate coefficients for the excitation processes⁴⁵



and



The rate coefficients for these three processes, at 3200 K, are 8.46×10^{-10} cm³/s, 9.35×10^{-10} , and 3.02×10^{-9} . In modified Arrhenius form, they were given as

$$k_{\text{excit}}(\text{K}) = 1.4 \times 10^{-8} T^{0.4} \exp(-38.3/RT),$$

$$k_{\text{excit}}(\text{Rb}) = 2.6 \times 10^{-8} T^{0.3} \exp(-36.5/RT),$$

and

$$k_{\text{excit}}(\text{Cs}) = 2.2 \times 10^{-8} T^{0.4} \exp(-33.1/RT).$$

(Rate coefficients are in cm³/s and activation energies, in kcal/mol.) We can only say that our rate constants appear to have values quite consistent with the excitation rate constants.

F. Collisional dissociation

The collisional dissociation rates k_1 and k_2 for the processes



and



respectively, were obtained for the eight salts NaCl, RbCl, CsCl, NaBr, KBr, RbBr, CsBr, and CsI. The values of the constants A and E in the expression

$$k = AT^{-7/2} \exp(-E/kT),$$

as well as the constants k_1 and k_2 for collisional dissociation

to ions and to atoms, respectively, are collected in Table V. This table also includes values obtained by Luther, Troe, and Wagner¹¹ where they are available.

Our data are most complete and reliable for RbCl, RbBr, CsCl, and CsBr. Cesium iodide presented experimental difficulties because of the low concentrations of I⁻ at equilibrium, when the total molecular concentrations were low enough to assure that molecule-molecule processes could be neglected. The same problem prevented us from studying rates of dissociation of the other iodides and the salts of sodium, with the exception of NaCl (and, to a rougher degree, NaBr).

Some of the species deserve individual comment. The NaBr and NaCl results were not fit on the analog computer; in these cases, the initial slopes of the curves for Na⁰ and halide were used to estimate k_1 and k_2 with the data from three shocks. These results are included in Table V.

Potassium bromide results are somewhat scattered, and the rate coefficient k_2 appears to be "anomalously" low at higher temperatures, as though the system shows more ionic branching as T increases.

Rubidium chloride has unusually low activation energies, especially for production of ions. In fact, a plot of $\ln k_2$ vs T^{-1} has a positive slope, because the $T^{-7/2}$ factor actually dominates the exponential. Like KBr, RbCl seems to branch more readily toward ions as the temperature increases.

The three cesium salts give us an opportunity to com-

TABLE V. Rate coefficients, activation energies, and preexponential factors for collisional dissociation of alkali halide molecules by argon.

Reaction	T (K)	k (cm ³ /s)	A (cm ³ deg ^{7/2} s ⁻¹)	E (kcal)	Reference (this work except where noted)
NaCl→Na ⁺ + Cl ⁻	3320	8.5×10^{-17} 2.3×10^{-15}		80	Refs. 7, 11
NaCl→Na ⁰ + Cl ⁰		2.6×10^{-15}			
NaBr→Na ⁺ + Br ⁻	3200	10^{-16}			
NaBr→Na ⁰ + Br ⁰		5×10^{-15}			
KBr→K ⁺ + Br ⁻	3000	1.5×10^{-15}	121	65	
KBr→K ⁰ + Br ⁰	3020	7.2×10^{-16}	6.0	46.9	
RbCl→Rb ⁺ + Cl ⁻	2700	1.1×10^{-15}	0.87	35.9	
RbCl→Rb ⁰ + Cl ⁰		3.3×10^{-15}	0.078	16.9	
RbCl→Rb ⁺ + Cl ⁻	4000	2.4×10^{-15}			
RbCl→Rb ⁰ + Cl ⁰		2.3×10^{-15}			
RbBr→Rb ⁺ + Br ⁻	3270	3.0×10^{-15}	8.4	47.1	
RbBr→Rb ⁰ + Br ⁰		3.7×10^{-15}	1.04	32.1	
CsCl→Cs + Cl ⁻	3200	2.4×10^{-15} 3.7×10^{-16}	4.1	47.8 100	Ref. 11
CsCl→Cs ⁰ + Cl ⁰		1.6×10^{-15}	6.2	48.6	
CsBr→Cs ⁺ + Br ⁻	2700	1.1×10^{-15} 5×10^{-14}	9.8	48.6 (10.4 inferred)	Ref. 11
CsBr→Cs ⁰ + Br ⁰	2800	8.0×10^{-16}	7.4	50	
CsBr→Cs ⁺ + Br ⁻	4200	6×10^{-15} 1×10^{-13}			Ref. 11
CsBr→Cs ⁰ + Br ⁰	4000	3.4×10^{-15}			
CsI→Cs ⁺ + I ⁻	2400	1.1×10^{-15} 8.3×10^{-16}			Ref. 11
CsI→Cs ⁰ + I ⁰	< 3000	< 10^{-18}			
CsI→Cs ⁺ + I ⁻	4000	2.2×10^{-14} $\sim 10^{-16}$			

*The third body, argon, has not been written explicitly here.

pare our values of the rate coefficients with an independently determined set. Luther, Troe, and Wagner¹¹ determined the extinction of shock-heated alkali halides in argon, at two or more wavelengths, in order to determine the concentrations of MX and X⁻. They assumed that the kinetics could be described, in essence, by reactions (1), (2), and (3). Reactions (5) and (6) were omitted from their model. The data were expressed in terms of a total bimolecular dissociation rate constant $k_{A\text{Hal}}$, the fraction γ dissociating to ions, and bimolecular detachment rate constant k_{Hal} . The rate constants $\gamma k_{A\text{Hal}}$, $(1 - \gamma)k_{A\text{Hal}}$ and k_{Hal} would be equivalent to our k_1 , k_2 , and k_3 , respectively, if we were to set k_5 , k_6 , k_7 , and k_8 to zero.

Our results for the rate coefficients k_1 and k_3 are in rather good agreement with the same rate coefficients as determined by Luther, Troe, and Wagner. Moreover we have determined the relative maximum ion concentration, as defined by these authors,¹¹

$$y = [\text{X}^-]_{\text{max}} / [\text{MX}]_{\text{initial}},$$

and again find good agreement. At 2400 K, Luther, Troe, and Wagner find Y of 10%–15%, and we find $Y = 10\%$ at 2800 K, and 20% at 3000 K. Despite this agreement, we draw very different inferences regarding the branching ratio k_2/k_1 , which we shall discuss shortly. We find that this ratio must be less than about 10^{-2} , corresponding to $\gamma \cong 1$, to be consistent with our data on Cs⁰, I⁻, and CsI, over the entire temperature range we studied. Luther, Troe, and Wagner infer from their model that their parameter $\gamma = 0.3$, or that the branching ratio $k_2/k_1 = 2.33$.

Our results with cesium bromide and cesium chloride also differ from those of Luther, Troe, and Wagner. We obtain branching ratios of about 0.6 for both salts, while the Lausanne–Göttingen group finds a ratio k_2/k_1 of approximately zero for CsBr, and two alternative values for this ratio for CsCl, either a value of approximately zero, or a value between 1.0 and 2.3. They choose the value zero—which is certainly the choice most consistent with our own previous work.¹

In the case of CsBr, Luther, Troe, and Wagner report values of Y , the maximum relative ion yield, of 30% at 2800 K and 60% at 4000 K. We find only 6% at 2800 K and 11% at 4000 K. This difference could be due, at least in part, to the relatively low value of the absorption cross section for Br⁻ in the wavelength region in which Luther, Troe, and Wagner measured the absorption by Br⁻. Our concentration measurements were made near the threshold wavelength for Br⁻, but far enough from it that the absorption by Br⁻ was strong. Moreover our concentrations measurements were followed to equilibrium and are consistent with the equilibrium concentrations of the other species, so long as we use the oscillator strengths derived to establish this self-consistency as described in the appendix. The rate coefficients and the activation energy, seem more consistent with the general pattern for the alkali halides than do the rather higher rate coefficients of Luther, Troe, and Wagner, and the very low activation energy that we infer from their rate coefficients. On the basis of the data of these experiments, we also cannot reconcile their low value of k_2/k_1 with our observations of the rise of Cs⁰ absorption at early times. Typically, the initial

slope of the Cs⁰ curve that we observed is roughly twice that of the Br⁻ curve, as the higher-temperature dissociation rates for CsBr indicate in Table V. These comparisons are treated further in Ref. 18.

In the case of cesium chloride, Luther, Troe, and Wagner again had the problem of inferring the molecular concentrations from data in which the halide ion dominated the absorption. The second-order rate coefficient for the decay of the absorption at the four wavelengths of their measurement was found to be 3.7×10^{-16} cm³/s at 3200 K, with an activation energy of 100 kcal/mol. The inference was then made that this rate is the dissociation rate k_1 . If this is accepted together with their analysis of the CsBr data, then Luther, Troe, and Wagner appear to obtain a ratio

$$\frac{k_1(\text{CsBr}, 2700 \text{ K})}{k_1(\text{CsCl}, 3200 \text{ K})} = 135,$$

which is rather difficult to understand. Our model leads us to

$$\frac{k_1(\text{CsBr})}{k_1(\text{CsCl})} = \frac{2.6 \times 10^{-15}}{2.4 \times 10^{-15}} = 1.08 \text{ at } 3200 \text{ K}.$$

G. Branching ratios

To interpret the branching problem, we found it useful to introduce the variable

$$b = k_2/k_1.$$

This quantity is the direct measure of the branching ratio for formation of atom pairs vs formation of ion pairs and is to be preferred over the observable variable we were previously¹ forced to use,

$$B(0) = \lim_{t \rightarrow 0} B(t) = \lim_{t \rightarrow 0} [\text{M}^0(t)] [\text{X}_{\text{eq}}^-] / [\text{M}_{\text{eq}}^0] [\text{X}^-(t)].$$

The desideratum b can only be evaluated by carrying out a kinetic model, such as we have described here.

The branching ratio b is as explicit a specification as one could ask to specify the degree of disequilibrium generated in the primary dissociation process. It is useful to compare the values of b with the square root of the corresponding equilibrium constant

$$K_5 = \frac{[\text{M}^0]_{\text{eq}} [\text{X}^0]_{\text{eq}}}{[\text{M}^+]_{\text{eq}} [\text{X}^-]_{\text{eq}}} \\ = 8 \exp[Q/kT] + 4 \exp[(Q - \Delta)/kT].$$

We have set $Q = \text{I.P.}(\text{M}^0) - \text{E.A.}(\text{X}^0)$ and Δ is the fine structure splitting of the halogen atom (0.1092, 0.4568, and 0.9424 eV for Cl, Br, and I, respectively). Insofar as free electrons can be neglected at early times, $K_5^{1/2}$ would be the value assumed by b if collisional dissociation produced a distribution of separated pairs equivalent to the thermally equilibrated distribution. There is, of course, no reason to expect b to have the same value as $K_5^{1/2}$; we make the comparison to give a quantitative sense of the degree of disequilibrium generated in this system. Values of b and $K_5^{1/2}$ are presented in Table VI. We have also included values of the parameter $B(0)$, and of the parameter γ introduced by Luther, Troe, and Wagner,¹¹ which is simply related to b : $b = \gamma^{-1} - 1$.

Taken together, the branching ratios seem to make a

TABLE VI. Branching ratios b , equilibrium constants $K_s^{1/2}$, initial branching concentrations $B(0)$, and fractions γ of dissociation to ions, for alkali halide dissociation.

Salt	$T(K)$	b	$K_s^{1/2}$ at (3000 K)	$B(0)$	γ	Source (this work except where noted)
NaCl	3320	32	60.1	0.51	0.03	
NaBr	3200	49	88.1	0.47	0.02	
KBr	3000	0.47	18.7	0.016	0.68	
RbCl	2700	3.2	9.37	0.25	0.24	
	4000	1	7.29	0.039	0.51	
RbBr	3270	1.2	13.7	0.044	0.45	
CsCl	3200	0.66	5.35	0.073	0.6	
		0			1	Ref. 7, 11
CsBr	2700	0.59	7.85	0.050	0.63	
		0			1	Ref. 7, 11
	4200	0.61	6.28 (4000 K)	0.022	0.62	
		0			1	Ref. 7, 11
CsI	2400	0	13.5	0	1	
		2.3		0.3		Ref. 7, 11

rather consistent picture, with the possible exception of the value for KBr. As we noted previously, the dissociation rate to atoms k_2 seems anomalously low for this species and should be taken with some skepticism. The other values provide a pattern in which all the molecules in this study dissociate to give distributions favoring the production of ions, relative to the distribution at thermal equilibrium. The salts vary from NaCl, in which b is about half of $K_s^{1/2}$, to the cesium salts, in which b is an order of magnitude less than $K_s^{1/2}$. If dissociation occurred purely statistically, then one would expect b to be $\sqrt{12}$ or 3.46; any value of b less than 3.46 corresponds, at least in a crude sense, to a negative temperature. Any value of b less than unity, of course, corresponds to an absolute preponderance of ions generated in the primary dissociation step.

We see that the statement made in Ref. 1, that the alkali halides "appear to span the full range of behavior, from the extreme of complete dissociation to ions,..." is itself probably too extreme, with the possible exception of CsI. The relatively fuller treatment of the entire kinetic system has clarified the way the alkali halides dissociate, and has shown that the "more ionic salts" do tend to dissociate to ions, rather than to atoms. This treatment has put the branching onto a quantitative basis. Furthermore, the analysis shows that the principal relaxation processes can be consistently accounted for in terms of three dominant reactions (and their reverse processes): collisional detachment of electrons from negative ions by the heavy particles of the heat bath, collisional ionization of the alkali atoms by electrons, and mutual ion-ion charge neutralization.

The question remains open to whether the branching ratios of Table VI are due to uncertainties in the data, to characteristics of the curve-crossing process, or to the kinetics of vibrational excitation in dense gases, or of all three. It will hopefully be possible to measure branching ratios for single-collision dissociation in extensions of the crossed beam studies that have already been carried out. Presumably, if these measurements are made for molecules having

progressively higher vibrational temperatures, the branching ratios should tend to resemble those of Table VI. The results of shock experiments on Rb and Cs halides at temperatures between 3000 and 6000 K are compatible with those of Table VI.¹⁸

In principle, it would seem possible to carry out simple studies of alkali atoms colliding with halogen atoms. Such measurements would merge with ours if differential cross sections, especially for negative ion production, were made at large scattering angles. Unfortunately the easier low-angle scattering measurements simply do not probe the same part of the potential as the dissociation experiments.

There remain the possibilities of spectroscopic studies, especially of NaI, whose many-line spectrum is known to exhibit a variety of linewidths.^{2,46} This study has recently become tractable because of the studies done on the fluorescence excitation and emission spectra of NaI.^{47,48} The shock tube method has been fairly fruitful, but is rapidly reaching the boundaries of its capabilities because of its limited time resolution; with a tube much larger than the one described here, one could hope to see the early-time behavior more clearly. In this way, one would try to satisfy the nagging doubt that there might yet be a short induction period after dissociation, before neutral atoms are present. However the force of the kinetic model is fairly compelling, and we now believe that any interpretation of the curve crossing problem in high-density systems must be compatible with the branching ratios we report here in Table VI, and with the more extensive results of Ref. 18.

ACKNOWLEDGMENTS

We would like to thank Gilbert Shaw for suggesting that we use the analog computer, Dr. L. S. Skaggs for allowing us to use it, and Robert Schreiner for helping to set up the calculations. This work was supported by a Grant from the U. S. Army Research Office, Durham, and in part by Public Health Service Research Grant 2 RO1 CA 06475, from the National Cancer Institute.

APPENDIX: ABSORPTION COEFFICIENTS OF MX AND M⁰

In the process of scaling the experimentally determined concentrations of MX and M⁰, we had the opportunity to measure, for each shock, the oscillator strength of the neutral alkali and the absorption cross section of alkali halide salt. The determinations were ultimately based entirely on the use of the halide ion absorption cross sections, which are known to $\sim \pm 30\%$. The oscillator strengths were calculated from the following equation:

$$f = \frac{2.608 \times 10^{12}}{l [M^0]_{\text{eq}}} \int \log \frac{I_0}{I_{\text{eq}}} d\nu,$$

where $(\log I_0/I)_{\text{eq}}$ is the equilibrium optical density of the alkali line, l is the path length (36 cm), and $[M^0]_{\text{eq}}$ is the equilibrium alkali concentration.

The molecular absorption cross sections were calculated from the equation

$$\sigma = \frac{1}{l' \Delta} \left[\ln \frac{I(0)}{I(\infty)} + \frac{1}{4} \text{OD}(X^-)_{\text{eq}} \frac{\sigma_s(X^-)}{\sigma_L(X^-)} \right],$$

where $\Delta = [MX]_0 - [MX]_{\text{eq}}$ and $[MX]_0$ and $[MX]_{\text{eq}}$ are the initial and equilibrium salt concentrations, l' is the path length (9 cm), $I(0)$ is the attenuated intensity of the Xe lamp before dissociation occurs, and $I(\infty)$ is the intensity at $t = \infty$. The bandpass of our interference filter was ~ 300 Å. In order to compare our results with those of Davidovits and Brodhead,¹⁹ their cross sections were averaged over the band pass of the filter in the following manner:

$$\bar{\sigma}_{\text{DB}} = \frac{\int_{\text{band pass}} \sigma_{\text{DB}}(\lambda) F(\lambda) L(\lambda) d\lambda}{\int_{\text{band pass}} F(\lambda) L(\lambda) d\lambda},$$

where $F(\lambda)$ is the transmission of the filter, $\sigma_{\text{DB}}(\lambda)$ is the molecular absorption cross section as a function of wavelength as determined by Davidovits and Brodhead. $L(\lambda)$ is the relative lamp intensity.

The molecular absorption cross sections offer no problem; most values agree within a factor of two of the previous results.¹⁹ However our alkali oscillator strengths are consistently lower than those found in the literature. Only the recent theoretical values computed by Weisheit⁴⁹ and some of the extrapolated values of Marr and Creek⁵⁰ are consistently close to our measured values. (The experimental values obtained by Korff and Breit²⁵ in 1932 are also similar to ours, but it is not clear whether these pioneering results can be credited with numerical accuracy, in view of the many pitfalls of absolute intensity measurements that are now recognized.) We would naturally like to interpret the general (albeit still rough) agreement between our experimentally determined oscillator strengths and Weisheit's calculated f values as an indication both of the correctness of the values and of the methods: in Weisheit's case, of the manner of treating core polarization and spin-orbit interaction, and in our case, of setting the condition of self-consistency.

Generally, the major uncertainty in oscillator strength measurements is due to the determination of concentrations. In our case the relative uncertainty in f can be written as

$$\frac{\delta f}{f} = \frac{\delta M_{\text{eq}}^0}{M_{\text{eq}}^0} + \frac{\delta \text{OD}(M_{\text{eq}}^0)}{\text{OD}(M_{\text{eq}}^0)}.$$

Since the determination of $[M^0]_{\text{eq}}$ from thermodynamic considerations is based on the value used for X_{eq}^- , let us assume that

$$\frac{\delta [M_{\text{eq}}^0]}{[M_{\text{eq}}^0]} \approx \frac{\delta [X_{\text{eq}}^-]}{[X^-]_{\text{eq}}} + \Delta,$$

where Δ is the uncertainty due to temperature. As a conservative estimate we take $\delta X^-/X \approx 0.25$ and $\delta \text{OD}(M^0)/\text{OD}(M^0) \approx 0.20$. The residual fractional uncertainty Δ can be estimated by calculating f numbers at two different temperatures. It is ~ 0.15 . The total expected uncertainty is thus $\sim 60\%$ which is consistent with our results.

Since the halide absorption cross sections are known to within 30%, there is, at most, a systematic error of 30% arising from this source. It is difficult to see where any additional systematic source of error could make a difference sufficient to bring our results into agreement with those in the literature.

The experimental values of Kvater and Meister,²⁶ and Gol'dberg²⁷ (based on the hook method) also depend on the accuracy of concentration or vapor pressure determinations. Since the vapor pressure is an exponential function of T , the measurement and constancy of temperature plays a crucial role in their results. It would be helpful if new, independent measurements of some of the oscillator strengths of the higher members of the alkali principal series could be measured with heat pipe ovens.

The question arises as to the optical thickness of the alkali lines. This problem is discussed in detail in Ref. 18. The conclusions of the extensive analysis carried out in that work are that the concentrations of alkali reported here are accurate, well within the other uncertainties of the measurements, except in the highest temperature ranges of this work, where the concentrations estimated from the thickest lines based on Voigt profiles are of order 20% higher for Rb and 30% higher for Cs than concentrations based on the assumption of Beer's Law. The comparison of rate coefficients reported here for Rb and Cs salts and those based on the rejection of optical thinness is made in Ref. 18. No experiments were done to determine the effect of optical thickness for NaCl, NaBr or KBr, but weak, high-lying transitions were used to monitor Na⁰ and K⁰, and no high-temperature results are reported here for these salts, the most refractory of those included in this study.

¹J. J. Ewing, R. Milstein, and R. S. Berry, *J. Chem. Phys.* **54**, 1752 (1971).

²R. S. Berry, in *Alkali Halide Vapors: Structure, Spectra, and Reaction Dynamics*, edited by P. Davidovits and D. L. McFadden (Academic, New York, 1979), Chap. 3.

³R. S. Berry, *J. Chem. Phys.* **27**, 1288 (1957).

⁴R. A. Berg and G. W. Skewes, *J. Chem. Phys.* **51**, 5430 (1960).

⁵M. Oppenheimer and R. S. Berry, *J. Chem. Phys.* **54**, 5058 (1971).

⁶R. S. Berry, T. Cernoch, M. Coplan, and J. J. Ewing, *J. Chem. Phys.* **44**, 127 (1968).

⁷V. R. Hartig, H. A. Olschewski, J. Troe, and H. G. Wagner, *Ber. Bunsenges. Phys. Chem.* **72**, 1016 (1968).

⁸A. Mandl, E. W. Evans, and B. Kivel, *Chem. Phys. Lett.* **5**, 307 (1970); A. Mandl, B. Kivel, and E. W. Evans, *J. Chem. Phys.* **53**, 2363 (1970).

- ⁹A. Mandl, *J. Chem. Phys.* **55**, 1918 (1971).
- ¹⁰A. Mandl, *J. Chem. Phys.* **55**, 2922 (1971).
- ¹¹K. Luther, J. Troe, and H. G. Wagner, *Ber. Bunsenges. Phys. Chem.* **76**, 53 (1972).
- ¹²A. Mandl, in *Alkali Halide Vapors: Structure, Spectra, and Reaction Dynamics*, edited by P. Davidovits and D. L. McFadden (Academic, New York, 1979), Chap. 12.
- ¹³F. P. Tully, Y. T. Lee, and R. S. Berry, *Chem. Phys. Lett.* **9**, 80 (1971).
- ¹⁴L. G. Piper, L. Hellemans, J. Sloan, and J. Ross, *J. Chem. Phys.* **57**, 4742 (1972).
- ¹⁵F. P. Tully, N. H. Cheung, H. Haberland, and Y. T. Lee, *J. Chem. Phys.* **73**, 4460 (1980).
- ¹⁶J. Ewing, Doctoral Dissertation, University of Chicago, 1970.
- ¹⁷R. Milstein, Doctoral Dissertation, University of Chicago, 1972.
- ¹⁸J. Weber and R. S. Berry, *Adv. Chem. Phys.* (in press).
- ¹⁹P. Davidovits and D. C. Brodhead, *J. Chem. Phys.* **46**, 2968 (1967).
- ²⁰S. Brodersen, *J. Opt. Soc. Am.* **43**, 877 (1953).
- ²¹S. Brodersen, *J. Opt. Soc. Am.* **44**, 22 (1954).
- ²²B. Steiner, M. L. Seman, and L. M. Branscomb, *J. Chem. Phys.* **37**, 1200 (1962).
- ²³B. Steiner, M. L. Seman, and L. M. Branscomb, in *Atomic Collision Processes*, edited by M. R. C. McDowell (North-Holland, Amsterdam, 1964), p. 537.
- ²⁴D. E. Rothe, *Phys. Rev.* **177**, 93 (1969).
- ²⁵S. A. Korff and G. Breit, *Rev. Mod. Phys.* **4**, 471 (1932).
- ²⁶G. Kvater and T. Meister, *Vestn. Lening. Univ.* **9**, 137 (1952).
- ²⁷G. I. Gol'dberg, *Izv. Gl. Astron. Obs.* **20** (156), 126 (1956).
- ²⁸O. S. Heavens, *J. Opt. Soc. Am.* **51**, 1058 (1961).
- ²⁹P. M. Stone, *Phys. Rev.* **127**, 1151 (1962).
- ³⁰D. G. Hummer, R. F. Stebbings, W. L. Fite, and L. M. Branscomb, *Phys. Rev.* **119**, 668 (1960).
- ³¹J. N. Bardsley, *Proc. Phys. Soc.* **91**, 300 (1967).
- ³²J. C. Y. Chen and J. L. Peacher, *Phys. Rev.* **167**, 30 (1968).
- ³³J. C. Browne and A. Dalgarno, *J. Phys. B* **2**, 885 (1969).
- ³⁴R. K. Janev and A. R. Tancic, *Proceedings Summer School and Symposium on Physics of Ionized Gases, Herceg Novi, 1970*, p. 7.
- ³⁵Yu. F. Bydin, *Sov. Phys. JETP* **23**, 23 (1966).
- ³⁶A. F. Haught, *Phys. Fluids* **5**, 1337 (1962).
- ³⁷Ya. B. Zel'dovich and Yu. P. Raizer, *Physics of Shock Waves and High Temperature Hydrodynamic Phenomena*, edited by W. D. Hayes and R. F. Probstein (Academic, New York, 1966).
- ³⁸L. G. Christophorou and J. A. D. Stockdale, *J. Chem. Phys.* **48**, 1956 (1968).
- ³⁹R. C. Slater, M. G. Fickes, and R. C. Stern, *Phys. Rev. Lett.* **29**, 333 (1972).
- ⁴⁰J. T. Moseley, W. Aberth, and J. R. Peterson, *J. Geophys. Res.* **77**, 255 (1972).
- ⁴¹J. Weiner, W. Peatman, and R. S. Berry, *Phys. Rev. A* **4**, 1824 (1971).
- ⁴²D. F. Dance, M. F. A. Harrison, and R. D. Rundel, *Proc. R. Soc. London Ser. A* **299**, 525 (1967).
- ⁴³D. R. Bates and M. R. Flannery, *Proc. R. Soc. London Ser. A* **302**, 367 (1968).
- ⁴⁴J. T. Moseley, R. E. Olson, and J. R. Peterson, *Case Stud. At. Phys.* **5**, 1 (1975).
- ⁴⁵F. R. Gilmore, E. Bauer, and J. W. McGowan, *J. Quant. Spectrosc. Radiat. Transfer* **9**, 157 (1969).
- ⁴⁶B. Schneider and R. S. Berry, unpublished (and still unassigned) high-resolution spectra taken through the courtesy of J. Lombardi and W. Klemperer, 1964.
- ⁴⁷A. S. Ragone, D. H. Levy, and R. S. Berry, *J. Chem. Phys.* **77**, 3784 (1982).
- ⁴⁸S. H. Schaefer, D. Bender, and E. Tiemann, *Chem. Phys. Lett.* **52**, 273 (1982).
- ⁴⁹J. C. Weisheit, *Phys. Rev. A* **5**, 1621 (1972).
- ⁵⁰G. V. Marr and D. M. Creek, *Proc. R. Soc. London Ser. A* **304**, 233 (1968).